

Lutein from Chicken Eggs Prevents Amyloid β -Peptide Aggregation In Vitro and Amyloid β -Induced Inflammation in Human Macrophages (THP-1)

Misuzu Matsui, Tomofusa Murata, Yuki Kurobe-Takashima, Tokuhei Ikeda, Moeko Noguchi-Shinohara, Kenjiro Ono, Hiroyuki Shidara, Kurataka Otsuka, Daisuke Kuriki, Michio Suzuki, and Shoko Kobayashi*



Cite This: *ACS Omega* 2024, 9, 26616–26627



Read Online

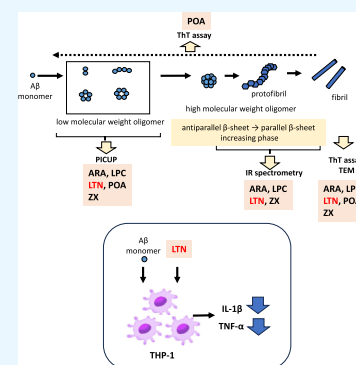
ACCESS |

Metrics & More

Article Recommendations

Supporting Information

ABSTRACT: Epidemiological studies predict that chicken eggs contain constituents other than proteins that prevent Alzheimer's disease. This study screened for constituents that inhibit the aggregation of amyloid β peptide ($A\beta$)_{1–42} and elucidated their mechanisms to explore the active components of chicken eggs. Thioflavin T assays and transmission electron microscopy observations showed that arachidonic acid (ARA), lysophosphatidylcholine, lutein (LTN), palmitoleic acid, and zeaxanthin inhibited $A\beta$ aggregation. Among these, ARA and LTN showed the highest activity. Photoinduced cross-linking of unmodified protein assays and infrared absorption spectrometry measurements showed that LTN strongly inhibited highly toxic $A\beta$ _{1–42} protofibril formation. Furthermore, LTN suppressed $A\beta$ _{1–42}-induced *IL1B* and *TNF* expression in human macrophage-like cells. In summary, LTN plays a crucial role in the AD-preventive effect of chicken eggs by suppressing $A\beta$ _{1–42} aggregation and $A\beta$ _{1–42}-induced inflammation.



1. INTRODUCTION

Globally, the number of individuals with dementia is significantly increasing. According to a report by the International Alzheimer's Association in 2021, there will be over 50 million people with dementia by 2020, and this number is expected to reach 152 million by 2050.¹ Alzheimer's disease (AD) is a progressive neurological disease that accounts for approximately 70% of dementia cases. Over 95% of patients have sporadic AD, and treatment after onset is difficult.² Currently, the drugs prescribed for AD can be classified into two categories based on their mechanism of action. (1) Acetylcholinesterase inhibitors (such as donepezil);³ (2) an NMDA-type glutamate receptor (NMDAR) antagonist (such as memantine).⁴ These medicines only delay or alleviate symptoms and are not expected to cure the disease. Moreover, side effects such as diarrhea and vomiting are frequently observed.^{2,5} Consequently, AD-targeting drugs have exceptionally low patient satisfaction compared to drugs targeting other diseases.

Therefore, novel anti-AD drugs were developed for this purpose. Among them, drugs targeting the amyloid hypothesis have attracted considerable attention. The idea that amyloid β peptide ($A\beta$) generated in the patient's brain triggers the pathological cascade of AD is called the "amyloid hypothesis" and is the most supported mechanism for the pathogenesis of AD. The accumulation of $A\beta$ in the brain is a characteristic AD pathology. A remarkable accumulation of $A\beta$, senile plaques, is observed in the brains of patients with AD. Depending on the

cleavage site of γ -secretase, $A\beta$ with 40 and 42 amino acid residues is mainly produced.⁶ The $A\beta$ monomers are soluble; however, they gradually form oligomers and further form insoluble protofibrils and mature fibrils.⁷ Monomers are not toxic, whereas oligomers are extremely toxic to the brain.⁸ $A\beta$ _{1–42} is less soluble in aqueous solution than $A\beta$ _{1–40}, and $A\beta$ _{1–42} causes fibrosis more readily. Therefore, $A\beta$ _{1–42} is easier to accumulate in the brain, and its relative amount increases with AD progression.⁹ $A\beta$ production and deposition are triggers of pathological cascade factors, including neurofibrillary changes due to tau hyperphosphorylation, leading to AD development. $A\beta$ deposition is thought to alter various intracellular signaling in AD brains, including increased caspase activity, reactive oxygen species production, elevated intracellular Ca^{2+} , and activation of the NF- κ B transcription factor.¹⁰ Neurofibrillary changes contribute to neuronal loss.¹¹ Furthermore, PS1, PS2, and APP were identified as multiple familial AD genes involved in $A\beta$ production.¹²

For over 10 years, anti-AD medicine was developed based on the amyloid hypothesis, such as γ -secretase inhibitors and $A\beta$ antibodies; however, most of them failed in clinical trials.

Received: April 9, 2024

Revised: May 10, 2024

Accepted: May 15, 2024

Published: June 3, 2024



However, Lecanemab (an anti- $A\beta$ monoclonal antibody developed by Eisai and Biogen) has recently attracted worldwide attention and was approved by the U.S. FDA in 2022 as a treatment for AD after it was shown to suppress cognitive decline in a phase III clinical trial.¹³ Meanwhile, clinical trials show that anti- $A\beta$ antibodies should be administered in the early stages of dementia, before AD onset.¹⁴ Lecanemab is intended for patients in the early stages of AD, when $A\beta$ accumulates in the brain. We focused on preventing $A\beta$ accumulation through daily dietary intake since it is important to prevent the accumulation of $A\beta$ in the brain before the onset of dementia.

Chicken eggs are a good food source for maintaining health due to their variety of nutrients. The human body utilizes chicken egg proteins due to their high amino acid score. Epidemiological studies suggest that chicken egg consumption reduces the risk of dementia.^{15,16} One study suggests that consuming chicken eggs might reduce the risk of developing dementia, and this effect is attributed to their high-quality protein.¹⁶ In addition, chicken egg proteins have various other functional properties. For example, ovalbumin in egg white shows antioxidant activity through amino acid residues such as cysteine and histidine on its surface when heated above 80 °C. Additionally, it enhances the inhibitory effects of linoleic acid (LNA) oxidation.¹⁷ In contrast, another study showed that chicken eggs reduced the risk of developing dementia only in the group that did not consume the Mediterranean diet.¹⁵ The proteins in chicken eggs showed no significant effect on the development of dementia. Eggs contain carotenoids and vitamins, which may also have a preventive effect on dementia.¹⁸

This study aimed to identify chicken egg components other than proteins that may have anti-AD effects. We screened 34 low-molecular-weight compounds in chicken eggs for their inhibitory effects on $A\beta$ aggregation using the thioflavin T (ThT) assay. We also investigated the inhibition of oligomerization and degradation of $A\beta$ fibrils using the components that showed activity in the screening. Five chicken egg constituents were identified as anti- $A\beta$ aggregation compounds. Lutein (LTN) strongly suppressed $A\beta$ aggregation and $A\beta$ -induced inflammation. Thus, LTN from chicken eggs may contribute to the prevention of AD.

2. MATERIALS AND METHODS

2.1. Reagents. The abbreviations for all compounds used for screening are shown in Table 1. L - α -Phosphatidylcholine (from egg yolk), cholesterol, stearic acid (SA), oleic acid (OA), LNA, L -glutamic acid, DL -methionine, L (+)-arginine, and taurine were purchased from Nakalai Tesque Corporation (Kyoto, Japan). Palmitic acid (PA), cyanocobalamin, and L -aspartic acid were purchased from Kanto Chemical Co. (Tokyo, Japan). L - α -Phosphatidylethanolamine solution (from egg yolk), phosphatidylinositol sodium salt (from wheat germ), L - α -lysophosphatidylcholine (from egg yolk), arachidonic acid (ARA), docosahexaenoic acid (DHA), LTN, zeaxanthin, retinol, β -carotene, (\pm)- α tocopherol, folic acid, sodium pantothenate, DL -threonine, L (+)-isoleucine, L -tryptophan, DL -phenylalanine, L (+)-lysine, and N -acetylneuraminic acid were purchased from Fujifilm Wako Pure Chemicals Corporation (Osaka, Japan). $A\beta_{1-42}$ was purchased from the Peptide Institute Inc. (Osaka, Japan). All other reagents were of the highest grade.

Table 1. Screening Constituents of Chicken Egg

constituents	classification
retinol (VA)	vitamin
β -carotene (β CAR)	
α -tocopherol (α -T)	
vitamin B12 (VB12)	
folate (FA)	
pantothenic acid (VBS)	
palmitic acid (PA)	fatty acid
palmitoleic acid (POA)	
stearic acid (SA)	
oleic acid (OA)	
linoleic acid (LNA)	
arachidonic acid (ARA)	
docosahexaenoic acid (DHA)	
lutein (LTN)	carotenoid
zeaxanthin (ZX)	
cholesterol (Cho)	lipid
sialic acid (NANA)	
aspartic acid (Asp)	free amino acid
threonine (Thr)	
serine (Ser)	
glutamic acid (Glu)	
methionine (Met)	
isoleucine (Ile)	
leucine (Leu)	
tyrosine (Tyr)	
phenylalanine (Phe)	
lysine (Lys)	
arginine (Arg)	
taurine (Tau)	
phosphatidylcholine (PC)	
phosphatidylethanolamine (PE)	
sphingomyelin (SM)	
phosphatidylinositol (PI)	
lysophosphatidylcholine (LPC)	

2.2. Screening for Egg Constituents That Prevent $A\beta$ Aggregation (ThT Assay). Thirty-four chicken egg components were screened by the ThT assay using a ThT β -Amyloid (1–42) Aggregation Kit (Anaspec, Inc., CA, USA). $A\beta_{1-42}$ was lyophilized, and 0.5 mg was dissolved in 2 mM NaOH, lyophilized, and dissolved in 20 mM phosphate buffer (1.9 mL, pH 7.4) prior to use. The final concentrations added to black 96-well plates were 100 μ M for the chicken egg constituent, 200 μ M for the ThT solution, and 50 μ M for the $A\beta_{1-42}$, respectively. Amyloid fibril formation was detected at 37 °C using a microplate and measuring fluorescence intensity at excitation (Ex)/fluorescence (Em) wavelengths = 440/484 nm every 5 min for 3 h using a plate reader (VARIOSKAN LUX, Thermo Fisher Scientific, MA, USA). The fluorescence intensity was expressed as relative fluorescence units (RFUs) by subtracting the blank value from the sample values. Phenol red (Phe red) was used as a positive control, and samples without egg constituents (only $A\beta_{1-42}$) were used as a negative control (NC).

The chicken egg constituents that inhibited $A\beta_{1-42}$ aggregation were further subjected to concentration-dependent studies conducted at 25 and 50 μM . The IC_{50} (50% inhibitory concentration) was calculated by sigmoidal curve fitting using GraphPad Prism software (version 10.0.3, GraphPad Software, Inc.).

The $A\beta$ fibril destabilization assay initially involved incubating $A\beta$ at 37 $^{\circ}\text{C}$ for 2 days to form fibrils. The RFU of ThT was subsequently measured for 1 h to confirm that the fluorescence reached stable states and $A\beta$ fibers were successfully formed (Figure S1). Five microliters of the active compounds (100 μM final concentration) were added to each well, and fluorescence measurements were performed for 5 h under the same conditions as the ThT assay.

2.3. Electron Microscopy. A 10 μL aliquot of each sample solution was spotted onto a copper grid (NISSHIN EM CO. Ltd., Tokyo, Japan) after performing ThT assays. The peptides were stained with 2% uranyl acetate in water, the solution was removed, and the grid was air-dried. Amyloid fibril formation was observed using a JEM-1010 transmission electron microscope (TEM, JEOL, Tokyo, Japan) at an acceleration voltage of 120 kV.

2.4. Chemical Cross-Linking and Determination of Oligomer Frequency Distributions. As previously described, photoinduced cross-linking of unmodified protein (PICUP) were performed to determine $A\beta$ small molecular oligomer formation.¹⁹ An overview of the PICUP apparatus is described in Figure S2. The apparatus was prepared according to a previous report.²⁰ A commercial flashlight was used as the light source, and a manual camera was placed in front of it. A small box was attached to a lens cap to allow the polymerase chain reaction (PCR) tube to stand. Eighteen microliters of $A\beta$ solution (25 μM final concentration) was added to the PCR tube containing 20 μL of chicken egg component solution (50 μM final concentration). One microliter of ammonium persulfate solution (1 mM final concentration) and 1 μL of tris(2,2'-bipyridyl) dichloro ruthenium(II) ($\text{Ru}[\text{bpy}]_3\text{Cl}_2$) (Sigma-Aldrich, MO, USA) solution (1 mM final concentration) was mixed by pipetting. $A\beta$ was immediately oligomerized by irradiation with 3000 lm of light from a flashlight for 1 s. The time was adjusted by using the shutter function of the camera. After irradiation, 2 μL of 80 mM dithiothreitol was added to immediately stop the reaction. Sodium dodecyl sulfate polyacrylamide gel electrophoresis (SDS-PAGE) and silver staining were performed as previously described to determine the frequency and distribution of monomers and oligomers.¹⁹ Briefly, 8 μL of each cross-linked sample was electrophoresed on a 10–20% polyacrylamide gradient tricine gel (Invitrogen, MA, USA) and visualized using a silver staining kit (SilverXpress, Invitrogen). Non-cross-linked samples were used as controls in each experiment. The gels were photographed using a LAS-4000 (GE Healthcare, IL, USA). ImageJ 1.54 software was used to quantify band intensity. The intensity of oligomers was defined as the sum of the normalized intensities of dimer, tetramer, pentamer, and hexamer in $A\beta_{1-42}$, and the ratio of oligomers was represented as the ratio of the NC group. The ratio of oligomers in each group was shown as means \pm standard error (SE).

2.5. Fourier Transform Infrared (FTIR) Spectroscopy. After the ThT assay, the sample solution (15 μL) was added to the attenuated total reflection (ATR) prism and dried at 25 $^{\circ}\text{C}$. This procedure was repeated twice. The integration time was 100 s, and the IR spectrum was measured from 1500 to 1700

cm^{-1} using an IRSpirit FTIR spectrophotometer (Shimadzu Corporation, Kyoto, Japan). A single-reflection diamond ATR accessory QATR-S (wideband specification) was used for detection.

2.6. Cell Culture and Differentiation of Human Microglia-like THP-1 Cells. The human monocytic cell line THP-1 was obtained from the JCRB Cell Bank, Osaka, Japan. THP-1 cells were maintained in Roswell Park Memorial Institute (RPMI)-1640 medium supplemented with 10% fetal bovine serum (FBS) and 1% penicillin/streptomycin (P/S). THP-1 cells were used after differentiation in all experiments to explore substantial changes in responsiveness during monocyte-to-macrophage differentiation. THP-1 cells (5×10^5 cells/mL) were seeded into 12-well culture plates and incubated with 100 nM paramethoxyamphetamine for 24 h to allow them to adhere to the plastic culture plates and develop a morphology of differentiated macrophages that most closely resembled microglia.

2.7. $A\beta$ Cytotoxicity Assays. The differentiated THP-1 macrophages were incubated in RPMI-1640 medium containing 10% FBS and 1% P/S at 37 $^{\circ}\text{C}$ for 24 h before stimulation. The cells were subsequently stimulated by adding 10 μM $A\beta_{1-42}$ for 24 h in the presence or absence of ARA, LPC, LTN, POA, and ZX. The concentrations that were nontoxic to the cells were determined based on the (3-(4,5-dimethylthiazol-2-yl)-2,5-diphenyltetrazolium bromide) (MTT) assay. After 24 h of incubation with chicken egg constituents, the supernatant was collected, and total RNA was extracted from the cells. The supernatant and total RNA were subjected to enzyme-linked immunosorbent assays (ELISA) and quantitative reverse transcription PCRs (RT-qPCRs), respectively.

2.8. MTT Assay. The MTT Cell viability Assay Kit was purchased from Cosmo Bio Co. Ltd. (Tokyo, Japan). THP-1 cells were seeded in 96-well plates at a density of 5×10^4 cells/well and cultured at 37 $^{\circ}\text{C}$ for 24 h. Subsequently, 100 μL of the medium containing 0, 0.1, 1, or 10 μM chicken egg constituent was added to the cells and incubated for 24 h. The MTT assay was performed following the manufacturer's protocol.

2.9. Quantitative RT-PCR. Total RNA was isolated from THP-1 cells using the TRIzol reagent (Invitrogen). Quantitative RT-PCR was performed by initially reverse transcribing 0.5 μg of purified total RNA using PrimeScript RT Master Mix (TaKaRa, Shiga, Japan), and the synthesized cDNA was amplified on the Thermal Cycler Dice Real Time System III (Takara) using TB Green Premix EX TaqII (TaKaRa). The primer sequences are listed in Table S1. Relative mRNA levels were normalized to glyceraldehyde-3-phosphate dehydrogenase (GAPDH) mRNA and expressed as fold changes.

2.10. ELISA. Interleukin 1 beta (IL 1 β) and tumor necrosis factor (TNF) levels were quantified using the Human IL-1 β ELISA kit (Proteintech, IL, USA) and the AuthentiKine Human TNF- α ELISA kit (Proteintech) according to the manufacturer's instructions. Absorbance was measured at 450 nm using a microplate reader (Molecular Devices, Sunnyvale, CA, USA), and sample concentrations (pg/mL) were calculated.

2.11. Statistical Analysis. Data are represented as means \pm SE. Statistical analyses were performed by repeated one-way or two-way ANOVA, followed by Dunnett's or Tukey–Kramer's tests; a p -value of under 0.05 was considered significant.

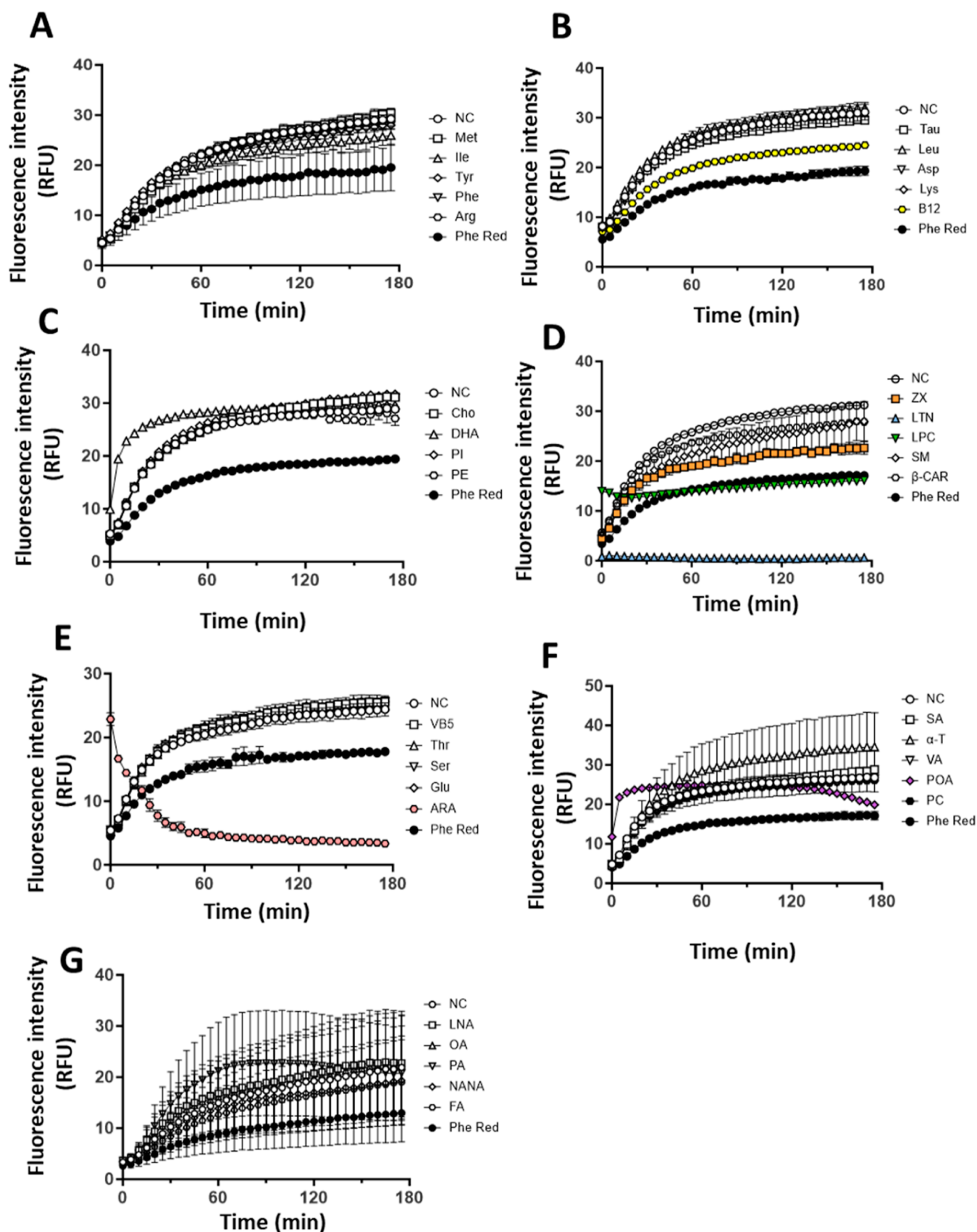


Figure 1. Screening of chicken egg constituents of $A\beta$ aggregation by ThT assays. ThT assays were performed to monitor the 3 h aggregation kinetics of $A\beta_{1-42}$ ($50 \mu\text{M}$) in the presence of $100 \mu\text{M}$ chicken egg constituents. Fluorescence spectroscopy was performed at an excitation wavelength of 440 nm and an emission wavelength of 490 nm. Values are represented as the mean \pm standard deviation ($n = 3$).

aggregation effect. Among these, the RFU of ARA and LTN were significantly reduced. Therefore, we further explored the inhibitory mechanisms of these five compounds. The RFU of POA, ZX, LPC, ARA, and LTN were suppressed, and ARA and LTN showed strong activity (Figure 2A). The structures of POA, ZX, LPC, ARA, and LTN are shown in Figure 2B.

The LTN (Figure 1D), ARA (Figure 1E), and LPC (Figure 1D) groups did not exhibit sigmoidal curves. LTN strongly inhibited $A\beta$ aggregation. ARA and LPC might show an $A\beta$ aggregation effect after incubating them with $A\beta$. ARA and LPC may physically interact with ThTs. Thus, we examined the anti- $A\beta$ aggregation effects of LTN, ARA, and LPC at lower concentrations to reduce their effect on ThT. The LTN group showed a sigmoidal curve at low concentrations (25 and 50 μM), whereas ARA and LPC did not improve (data not shown). Since this was considered a limitation of the ThT assay, its inhibitory activity was confirmed using TEM.

3.2. Comparison of the Activity of Chicken Egg Constituents. We calculated IC_{50} values of POA, ZX, LPC, ARA, and LTN that inhibit the aggregation of $A\beta_{1-42}$ to 50% of the NC value by sigmoidal curve fitting of the data (Figure S3). The IC_{50} of ARA and LTN were 37.4 and 74.0 μM , respectively (Figure 2C). The IC_{50} values for POA, ZX, and LPC could not be calculated since these compounds did not exhibit a 50% decrease within this concentration range. POA showed high activity at 25 and 50 μM , and 100 μM of POA had the lowest activity (Supplemental Figure 3). This indicated that POA showed no concentration dependence and had an optimum concentration. These results indicate that ARA and LTN have high activity and that POA has a different mechanism than that of the other compounds.

3.3. Observation of $A\beta$ Fibers Using TEM. We observed the $A\beta_{1-42}$ fibril using TEM after 3 h incubation with or without chicken egg constituents (Figure 2D). POA, ZX, LPC, ARA, and LTN inhibited $A\beta_{1-42}$ aggregation (Figure 2D). LTN inhibited the $A\beta_{1-42}$ aggregation the most; these results are consistent with the ThT assay. Meanwhile, the morphology of $A\beta$ fibrils with POA was amorphous, which differed from the other compounds.

3.4. $A\beta$ Oligomerization Assay. Low-molecular-weight $A\beta$ oligomers are formed in the first step of $A\beta$ aggregation (Figure 3A). The PICUP method determined whether POA, ZX, LPC, ARA, or LTN blocked this process; it is a rapid and efficient photochemical cross-linking method that requires no structural modification of $A\beta_{1-42}$ and accurately reveals the oligomerization state of $A\beta_{1-42}$.¹⁹ Only $A\beta_{1-42}$ monomers and trimers were observed without cross-linking (Figure 3B, NC without PICUP). Sodium dodecyl sulfate in the sample preparation solution induces a few artifacts of $A\beta_{1-42}$ trimer bands.^{19,20} $A\beta_{1-42}$ was comprised of monomers and oligomers of order 2–5 following cross-linking (Figure 3B). This is consistent with a previous report.¹⁹

All the five compounds inhibited oligomerization at 250 μM (Figure 3B,C). The intensities of the dimer, tetramer, tetramer, and pentamer bands were lower than those of the NC. Meanwhile, only POA and ZX inhibited oligomerization at final concentrations of 50 μM (Figure 3B,C).

These results indicated that POA, ZX, LPC, ARA, and LTN inhibited $A\beta_{1-42}$ fibril formation and oligomerization, and POA and ZX strongly inhibited them.

3.5. Inhibition of Formation of High-Molecular-Weight $A\beta$ Oligomers. The β -sheets of $A\beta$ increase as aggregation progresses.⁶ The secondary structure changes as

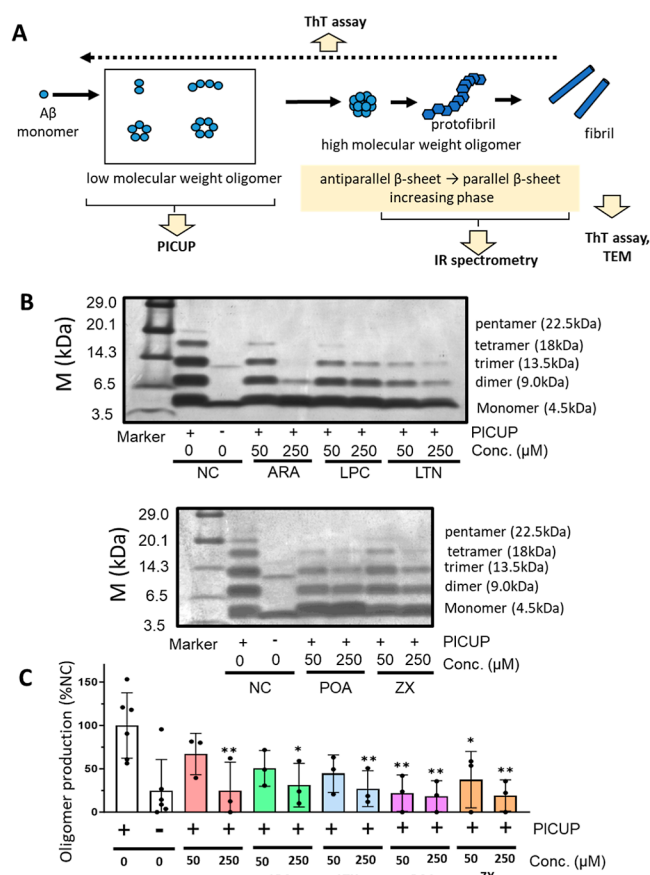


Figure 3. The effect of chicken egg constituents on $A\beta$ oligomerization. (A) The $A\beta$ aggregation scheme and assay system of each step. (B) Photo-induced cross-link unmodified proteins (PICUP), followed by sodium dodecyl sulfate polyacrylamide gel electrophoresis (SDS-PAGE) and silver staining, was used to determine the effects of 50 and 250 μM arachidonic acid (ARA), lysophosphatidylcholine (LPC), lutein (LTN), palmitoleic acid (POA), and zeaxanthin (ZX) on oligomerization of $A\beta_{1-42}$; +, with cross-linking; -, without cross-linking. (C) ImageJ and PICUP were used to quantify the intensity of each band following SDS-PAGE. The rate of oligomers was defined as the sum of the normalized intensities of dimer, tetramer, pentamer, and hexamer in $A\beta_{1-42}$. The intensity of oligomers in each group was shown as the mean \pm standard error when the intensity of oligomers in the NC group was 100. The data were represented as the mean \pm standard deviation ($n = 3$). Statistical analyses were performed using Dunnett's multiple comparison test ($*p < 0.05$; $**p < 0.01$).

the high-molecular-weight oligomer increases, and the β -sheet structure of $A\beta$ shifts from an antiparallel β -sheet to a parallel β -sheet.²¹ These structural changes were observed in the IR spectrum; thus, FTIR spectroscopy was performed (Figure 4A). The peak at 1639 cm^{-1} in the FTIR spectrum is specific for the parallel β -sheet of $A\beta_{1-42}$ protofibrils and fibrils. $A\beta_{1-42}$ incubated alone increased the peak area in the range of 1615–1645 cm^{-1} (Figure 4A). This is consistent with a previous report.²² The area under the curve (AUC) of the absorbances in the range of 1615–1645 cm^{-1} decrease when ARA, LTN, LPC, and ZX were mixed with $A\beta_{1-42}$, and LPC and LTN showed a particular decrease (Figure 3B). These results indicated that ARA, ZX, LPC, and LTN inhibited the formation of parallel β -sheet structures. The parallel β -sheet structure is only observed in high-molecular-weight oligomers such as protofibrils and fibrils. Therefore, our results suggested

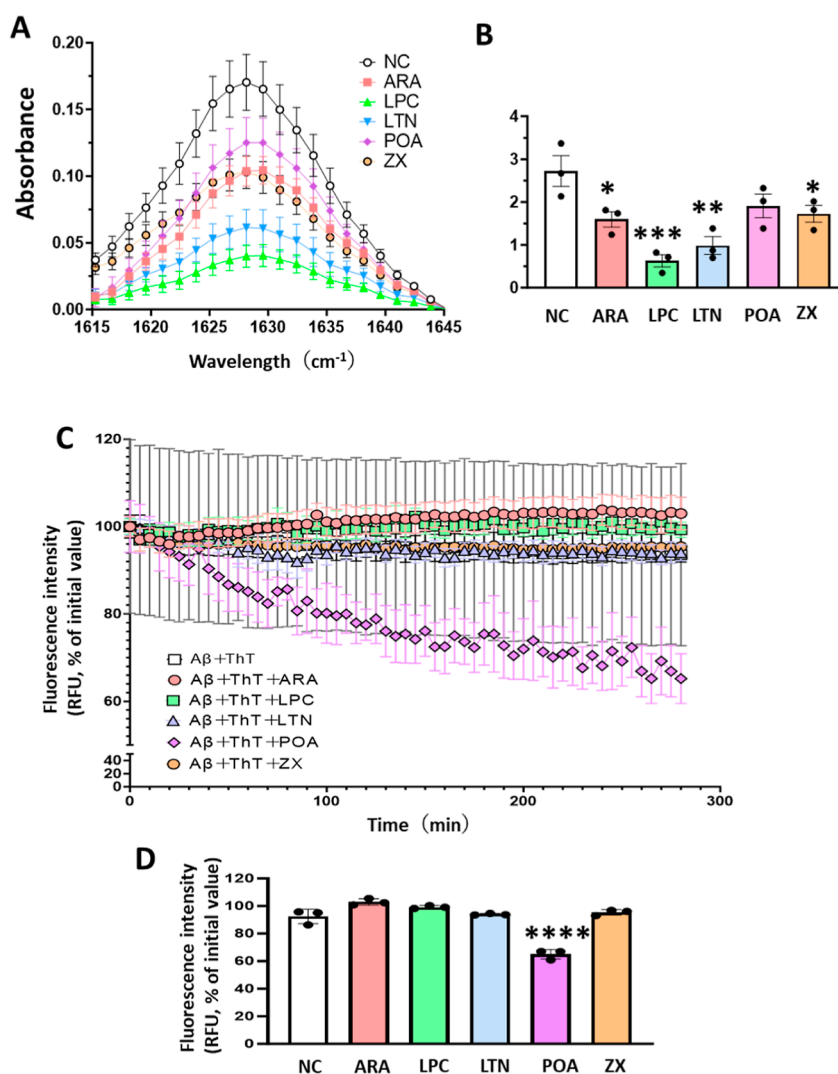


Figure 4. Effect on $A\beta$ secondary structure and destabilization of $A\beta$ fibrils. (A) FTIR spectrometry monitored the $A\beta_{1-42}$ secondary structure. The peak in the range of 1615–1640 cm^{-1} indicates a parallel β sheet structure. (B) We calculated the area under the 1615–1640 cm^{-1} absorbance curve. Values are expressed as the mean \pm standard deviation ($n = 3$). Statistical analyses were performed using Dunnett's multiple comparison test (* $p < 0.05$; ** $p < 0.01$). (C) Effects of chicken egg constituents on $A\beta_{1-42}$ fibril destabilization. The reaction mixtures containing 50 μM $A\beta_{1-42}$ and 100 μM of each chicken egg constituent were incubated at 37 $^{\circ}\text{C}$ for the indicated times. Values are the mean \pm standard deviation ($n = 3$) at all points. (D) AUC of the $A\beta_{1-42}$ fibril destabilization assay. Values are expressed as the mean \pm standard deviation ($n = 3$). Statistical analyses were performed using Dunnett's multiple comparison test (**** $p < 0.0001$).

that ARA, ZX, LPC, and LTN inhibited the formation of high-molecular-weight oligomers.

3.6. Fibril-Destabilizing Assay. POA, ZX, LPC, ARA, and LTN were incubated with $A\beta$ fibrils, and the RFU of ThT was monitored to examine whether they destabilize the $A\beta$ fibrils. The RFU of ThT remained unchanged during the incubation of $A\beta_{1-42}$ fibrils with ARA, LPC, LTN, and ZX or without additional constituents at 37 $^{\circ}\text{C}$ (Figure 4C,D). In contrast, the RFU of ThT decreased after the addition of POA to the fibrils (Figure 4C,D). These data indicated that POA could destabilize $A\beta_{1-42}$ fibrils.

3.7. Effect of Chicken Egg Constituents on $A\beta$ Toxicity in THP-1 Cells. Initially, an MTT assay was performed to determine the optimal concentrations of these chicken egg constituents (Figure S4). The final ARA, LPC, LTN, POA, and ZX concentrations were 0.1, 10, 0.1, 10, and 1 μM , respectively. The production of *IL 1B* and *TNF* mRNA increased when THP-1 cells were exposed to 10 μM $A\beta_{1-42}$

(Figure 5). LTN suppressed *IL 1B* and *TNF* mRNA and their corresponding proteins induced by $A\beta_{1-42}$.

4. DISCUSSION

Previous studies suggest that chicken eggs contain active constituents against AD other than proteins.¹⁸ We screened for free small molecular compounds in chicken eggs to identify the active constituents. ARA, LPC, LTN, POA, and ZX were identified as anti- $A\beta_{1-42}$ aggregation compounds in chicken eggs after screening using the ThT assay. These results were consistent with the TEM observation, reflecting the final $A\beta$ fibril formation. The inhibition mechanisms seemed to differ between the compounds because there was no common chemical structure. These active compounds were classified as fatty acids, phospholipids, and carotenoids (Table 1). We will discuss the inhibitory mechanisms of these five compounds for $A\beta$ fibril formation based on the ThT assay and TEM observation.

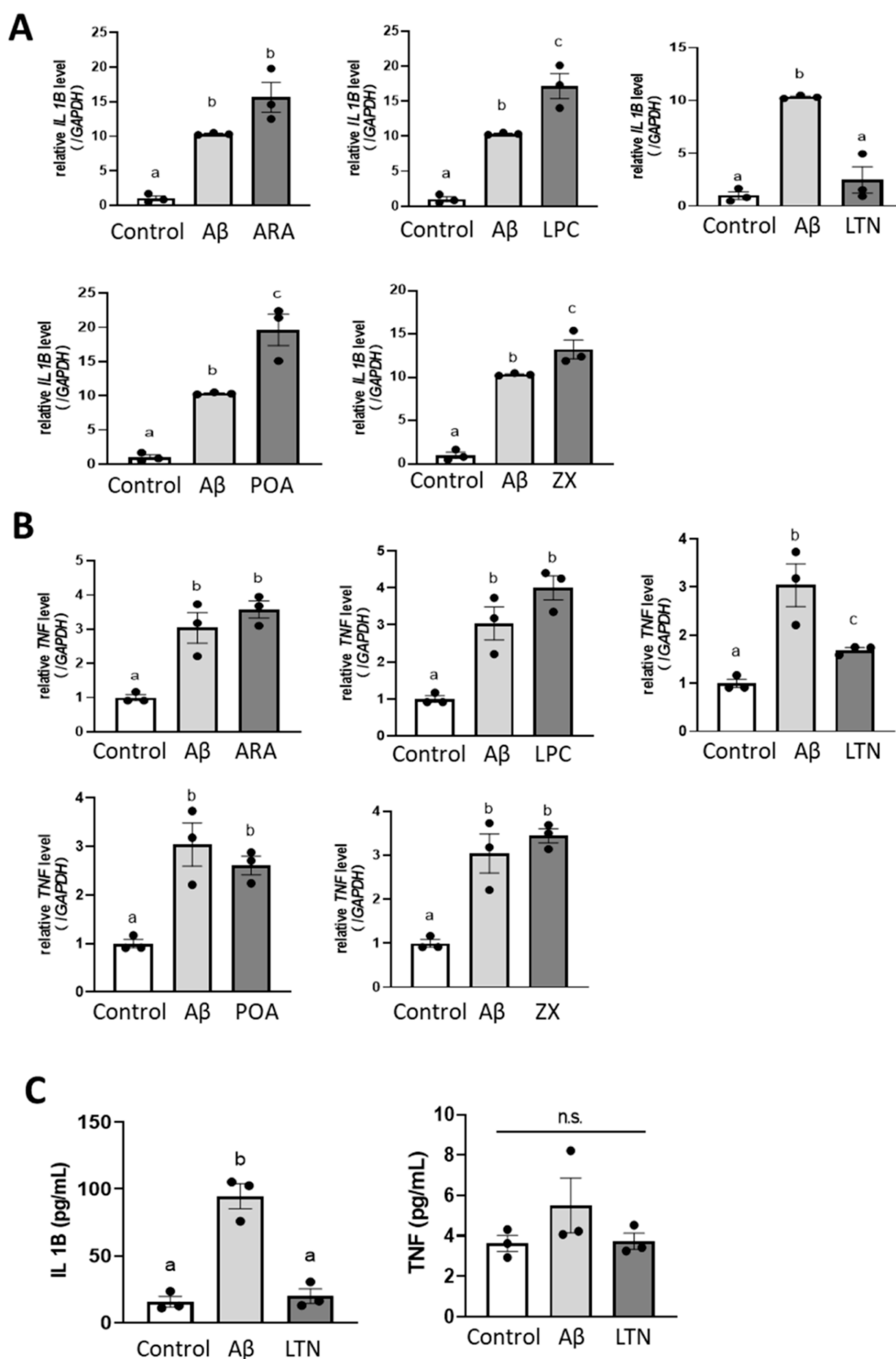


Figure 5. Effect of chicken egg constituents on $A\beta$ toxicity in THP-1 cells. THP-1 cells were treated with $A\beta_{1-42}$ and ARA (0.1 μ M), LPC (10 μ M), LTN (0.1 μ M), POA (10 μ M), or ZX (1 μ M) for 24 h, and TNF (A) and IL1 β (B) were measured using RT-qPCR. After treatment with LTN, the protein levels in the cell culture media were measured using a human-specific ELISA kit (C). Data are expressed as the mean \pm SE ($n = 3$). Statistical analyses were performed using Tukey's multiple comparison test. Different letters and asterisks indicate significant differences at $P < 0.05$.

Both fatty acids (ARA and POA) are unsaturated. The inhibitory activity of ARA on $A\beta$ fibril formation was the second highest among all the chicken egg constituents. The RFU of the ARA group in the ThT assay started at approximately 25, decreased in a time-dependent manner, and converged to a constant value (Figure 1E). This result led to the hypothesis that ARA initially served as a scaffold for $A\beta_{1-42}$ aggregation and temporarily promoted aggregation, inhibiting subsequent aggregation by interacting with each $A\beta$ binding site. The mechanisms underlying ARA inhibition were investigated in detail. El Shatshat et al. predicted the binding model of ARA to $A\beta_{1-42}$ oligomers using molecular docking simulation.²³ ARA is thought to bind to the groove region formed by the N- and C-terminal amino acid residues of $A\beta_{1-42}$. ARA binds linearly in the three-dimensional conformation of the $A\beta$ fibril. The hydrophobic structure of ARA is bound to leucine17 and leucine34, and the carboxyl group is bound to glutamine1. These docking simulation data support the ThT assay results.

The RFU of the POA group increased faster than that of the NC group in the ThT assay, and the RFU value gradually decreased until approximately 120 min after reaching saturation (Figure 1D). DHA is an unsaturated fatty acid that rapidly increases at the beginning. However, the RFU in the DHA group did not decrease after saturation. The TEM images showed that the $A\beta_{1-42}$ aggregates were amorphous (rather than fibrous) following POA addition (Figure 2D). This phenomenon was not observed for the other compounds, suggesting that POA's inhibitory mechanisms differed. Only POA destabilized the $A\beta_{1-42}$ fibril (Figure 4C). POA inhibited $A\beta$ oligomerization in the PICUP (Figure 3). These results suggest that POA may decrease $A\beta$ stability. To the best of our knowledge, this is the first report of the effect of POA on the $A\beta_{1-42}$ aggregates.

Analysis of LPC, PC, PE, PI, and SM phospholipids from chicken eggs showed that only LPC inhibited $A\beta_{1-42}$ aggregation when comparing the final RFU values. LPC is a lysophospholipid with a fatty acid that may favor its activity. Phospholipids are precursors of lysophospholipids that contain a polar headgroup and two hydrophobic fatty acid (hydrophobic) groups. In contrast, lysophospholipids contain one polar head and one fatty acid group. Therefore, lysophospholipids are relatively water-soluble and act as lipid mediators. $A\beta_{1-42}$ has hydrophilic and hydrophobic regions and may interact with LPC, which has more amphiphilic properties than phospholipids. The RFU of the LPC group remained almost constant from the initial value and did not show a sigmoidal curve (Figure 1D). $A\beta$ binds and is immobilized on lipid bilayers in the brain.²⁴ Consequently, $A\beta$ is restricted in diffusion and decreases (or sometimes increases) the aggregation rate.²⁵ Therefore, we hypothesize that the initial increase of RFU and subsequent stability in the LPC group may be due to LPC providing a scaffold for $A\beta_{1-42}$ in the early phase. One previous paper reported that LPC facilitates $A\beta_{1-42}$ aggregation.²⁶ These contradictory results may be due to the different experimental methods, such as incubation time, concentration, and reaction volume. In addition, the LPC effect of providing a scaffold for $A\beta_{1-42}$ may facilitate or prevent aggregation, depending on the situation. LPC might temporarily promote aggregation of $A\beta_{1-42}$ and subsequently restrict $A\beta_{1-42}$ diffusion to prevent aggregation.

We examined carotenoids (LTN, ZX, and β -CAR) in chicken eggs. LTN and ZX inhibited $A\beta_{1-42}$ aggregation, with

LTN exhibiting the highest inhibition among all chicken egg components (Figure 1D). LTN and ZX were previously shown to inhibit $A\beta$ aggregation.²⁷ However, to the best of our knowledge, no reports analyze which processes of $A\beta_{1-42}$ aggregation and flocculation are inhibited by these compounds (described below). LTN contains eight conjugated double bonds, including closed rings at both chain ends. Two hydroxyl groups on each side are important to inhibit $A\beta$ fibril formation.²⁷ These inhibitory activities of the carotenoid depended on the number of hydroxyl groups (LTN = ZX > β -CAR). ZX is a stereoisomer of LTN that only differs in the orientation of the hydroxyl group at the 3' position in cyclohexene; consequently, ZX inhibited $A\beta_{1-42}$ aggregation less than that of LTN. This indicated that the number of hydroxyl groups and their orientation are important for carotenoid activity.

As discussed, the ThT assay reflects the final $A\beta_{1-42}$ fibril production (Figure 2A,D), and ARA and LTN had the highest activity (Figure 2C). We examined which process of $A\beta_{1-42}$ aggregation was inhibited by the five active components (Figure 3A). Initially, the effect on the first step of $A\beta$ aggregation (low-molecular-weight oligomerization) was analyzed by PICUP. All five constituents inhibited oligomer formation at 250 μ M, whereas only POA and ZX were inhibitory at 50 μ M. This indicated that POA and ZX were more effective than the other three constituents in the initial stage. In contrast, POA and ZX showed lower inhibitory activity than ARA and LTN in the ThT assay (Figure 2A). POA and ZX may strongly inhibit oligomer formation and subsequently suppress $A\beta_{1-42}$ aggregation less than ARA and LTN. ARA and LTN are the most active in the ThT assay and did not inhibit oligomerization at 50 μ M. Thus, ARA and LTN may be more effective at inhibiting latter-stage oligomerization.

A unique β -sheet structure in amyloid aggregates was measured using FTIR spectroscopy to determine the effect of forming high-molecular-weight oligomers. Protofibrils are high-molecular-weight oligomers that are more toxic than $A\beta$ fibrils and strongly correlate with the onset of AD.¹³ Lecanemab is an antibody preparation recently approved as a new AD treatment medicine by the FDA, and it targets $A\beta$ protofibrils.¹³ Preventing the production of $A\beta$ protofibrils is important to prevent AD. ARA, LPC, LTN, and ZX decreased the peak in the range of 1615–1645 cm^{-1} , which is the specific band for the parallel β -sheet of $A\beta_{1-42}$ protofibrils and fibrils (Figure 4A). This suggested that the formation of protofibrils and fibrils was suppressed. The AUCs of the LPC and LTN groups were particularly low, suggesting that they strongly inhibited protofibril and fibril production.

Finally, we examined whether these five components inhibit inflammation induced by $A\beta_{1-42}$ using human microglia-like cells THP-1. Microglia are immune cells responsible for regulating inflammation and the phagocytosis of abnormal proteins such as $A\beta$ in the brain. Microglia activation begins at the same time as $A\beta$ accumulation, and their activation level increases as the pathology progresses in the brain of patients with AD.²⁸ Inflammatory stimulation (such as $A\beta$ accumulation and nerve damage) activates microglia. Two types of activated microglia exist: M1 and M2. The M1-activated microglia release inflammatory mediators such as IL 1B and TNF, which increase inflammation in the brain and cause neuronal cell death. We investigated the production of chemokines (IL 1B and TNF) induced by $A\beta_{1-42}$ in THP-1 cells and the ability of chicken egg constituents to inhibit them.

THP-1 cells were used because they possess many phenotypic and functional features and are widely used as models for human monocytes, macrophages, and microglia.²⁹ Human monocyte-derived macrophages share many phenotypic and functional features with human microglial cells and brain macrophages.³⁰ Thus, THP-1 cells were used after differentiation in all experiments to explore substantial changes in responsiveness during monocyte-to-macrophage differentiation. Initially, the optimal concentration of each compound was determined using an MTT assay (Supplemental Figure 4). The mRNA expression of *IL 1B* and *TNF* in THP-1 cells increased upon $A\beta_{1-42}$ addition.

The assay results revealed that LTN strongly suppressed the expression of *IL 1B* and *TNF* in THP-1 cells after $A\beta_{1-42}$ stimulation (Figure 5). The protein concentration of IL 1B in the supernatant was also suppressed; no difference was observed for TNF because the amount of TNF in the supernatant was considerably low. These TNF expression differences could be due to overtime mRNA and protein expression differences. In conclusion, LTN inhibited $A\beta$ fibril formation by suppressing the formation of initial oligomers and mature protofibrils. Additionally, it inhibited the $A\beta$ -induced release of inflammatory cytokines in THP-1 microglia, suggesting that LTN may be neuroprotective by suppressing $A\beta$ aggregation and inflammation in the brain.

Conversely, the expression levels of ARA, LPC, POA, and ZX were not suppressed. ARA exhibited high activity in the ThT assay; however, it is also an inflammatory mediator. $A\beta$ activates microglia, increasing the expression levels of cyclooxygenases COX-1 and -2, which metabolize ARA into inflammatory mediators during inflammation.³¹ Therefore, the addition of $A\beta_{1-42}$ to THP-1 cells possibly increased the expression levels of COX and induced the production of inflammatory mediators from ARA. However, ARA is essential for brain membrane integrity, and dietary intake of unsaturated fatty acids, such as ARA and DHA, is crucial for maintaining brain volume.³² POA destabilized $A\beta$ fibers but did not suppress inflammation in THP-1 cells. LTN showed activity in all assays except $A\beta$ fiber destabilization. Particularly noteworthy is its concentration-dependent and potent activity in the ThT assay and its strong inhibitory activity on protofibril formation, suggesting that inhibiting protofibril formation is crucial for suppressing inflammation in microglia. However, THP-1 cells are a tumor-derived cell line. Although they are differentiated, they serve as a surrogate model for studying compound effects, which is a limitation of this experiment.

The bioavailability of LTN is discussed since we observed that it is a crucial compound for inhibiting $A\beta$ aggregation and $A\beta$ -induced inflammation. LTN and ZX are not converted into vitamin A. The main sources of carotenoids in humans are green vegetables and egg yolks.³³ Although green vegetables contain more carotenoids, the intestinal permeability of animal products is higher than that of vegetables. Carotenoids in plant-based foods are crystalline aggregates, whereas those in animal-based foods are lipids.³⁴ The carotenoid composition of egg yolks depends on the composition of the hen's diet.³⁵ The intestinal absorption of carotenoids is significantly lower than that of other fat-soluble food components, such as lipids, fats, and vitamin E.³⁶ The reason for the low intestinal absorption of carotenoids in vegetables is that they are difficult to release from the cell wall and form the large solid-crystalline aggregates.³⁴ Carotenoids need to dissolve and spread in the digestive tract for absorption; thus, they must be initially

released from food. Carotenoids are easily released from animal products because of the absence of cell walls. LPC increases the intestinal absorption of LTN in vitro using an intestinal epithelial model (Caco-2 cells).³⁷ LTN from chicken eggs may be more bioaccessible than that from other foods since chicken eggs are an animal food that contains LPC. Because the concentration of LTN in the brains of monkeys increases after feeding,³⁸ LTN from chicken eggs may reach the human brain. Furthermore, chicken eggs are often cooked daily; LTN is heat-tolerant and thus considered stable for cooking. Therefore, the intake of LTN from chicken eggs is advantageous from the viewpoint of bioavailability efficiency and could directly inhibit $A\beta$ aggregation in the brain.

In conclusion, we observed LTN as an important constituent of chicken eggs that inhibits $A\beta$ aggregation and suppresses microglial inflammation. LTN in chicken eggs may have an anti-AD effect, together with the functions of other constituents. We emphasize that LTN might have high bioavailability when consumed from chicken eggs and strongly inhibits the formation of protofibrils, which is important to prevent AD, and it is possible to produce eggs with high functionality in the future since the amount of LTN in chicken eggs can be easily increased by adding it to chicken food.

■ ASSOCIATED CONTENT

Data Availability Statement

No data was used for the research described in the article.

Supporting Information

The Supporting Information is available free of charge at <https://pubs.acs.org/doi/10.1021/acsomega.4c03353>.

Stability of $A\beta$ fibrils before addition of chicken egg constituents, model of PICUP, concentration dependence of the ThT assay, concentration dependence of chicken egg constituents on cell toxicity and primer sequences used in this study (PDF)

■ AUTHOR INFORMATION

Corresponding Author

Shoko Kobayashi – Department of Applied Biological Chemistry, Graduate School of Agricultural and Life Sciences, The University of Tokyo, Tokyo 113-8657, Japan; orcid.org/0000-0003-1100-9011; Phone: +81-3-5841-5378; Email: ashokok@g.ecc.u-tokyo.ac.jp

Authors

Misuzu Matsui – Department of Applied Biological Chemistry, Graduate School of Agricultural and Life Sciences, The University of Tokyo, Tokyo 113-8657, Japan

Tomofusa Murata – Department of Applied Biological Chemistry, Graduate School of Agricultural and Life Sciences, The University of Tokyo, Tokyo 113-8657, Japan

Yuki Kurobe-Takashima – Department of Applied Biological Chemistry, Graduate School of Agricultural and Life Sciences, The University of Tokyo, Tokyo 113-8657, Japan; orcid.org/0000-0001-8756-8659

Tokuhei Ikeda – Department of Neurology, Kanazawa University Graduate School of Medical Sciences, Kanazawa 920-1192, Japan

Moeko Noguchi-Shinohara – Department of Neurology, Kanazawa University Graduate School of Medical Sciences, Kanazawa 920-1192, Japan

Kenjiro Ono – Department of Neurology, Kanazawa University Graduate School of Medical Sciences, Kanazawa 920-1192, Japan; orcid.org/0000-0001-8454-6155

Hiroyuki Shidara – R&D Division, Kewpie Corporation, Tokyo 150-0002, Japan

Kurataka Otsuka – R&D Division, Kewpie Corporation, Tokyo 150-0002, Japan; Division of Translational Oncology, Fundamental Innovative Oncology Core, National Cancer Center Research Institute, Tokyo 104-0045, Japan; Tokyo NODAI Research Institute, Tokyo University of Agriculture, Tokyo 156-8502, Japan; Division of Molecular and Cellular Medicine, Institute of Medical Science, Tokyo Medical University, Tokyo 160-8402, Japan

Daisuke Kuriki – R&D Division, Kewpie Corporation, Tokyo 150-0002, Japan; Division of Translational Oncology, Fundamental Innovative Oncology Core, National Cancer Center Research Institute, Tokyo 104-0045, Japan

Michio Suzuki – Department of Applied Biological Chemistry, Graduate School of Agricultural and Life Sciences, The University of Tokyo, Tokyo 113-8657, Japan

Complete contact information is available at:
<https://pubs.acs.org/10.1021/acsomega.4c03353>

Author Contributions

M.M. and T.M.: investigation, conceptualization, data curation, formal analysis, methodology, software, validation, visualization, writing—original draft, writing—review, and editing. **Y.K.-T.:** formal analysis, writing the original draft, writing the review, and editing. **T.I., M.N.-S., and K.O.:** formal analysis, conceptualization, resources, writing, review, and editing. **H.S., K.O., and D.K.:** funding acquisition, writing, review, and editing. **M.S.:** Data curation, formal analysis, methodology, writing the original draft, writing the review, and editing. **S.K.:** formal analysis, conceptualization, data curation, resources, supervision, investigation, methodology, writing—original draft, validation, visualization, writing—review and editing, funding acquisition, and project administration.

Funding

This research was supported by the Research Program on Development of Innovative Technology Grants from the Project of the Bio-oriented Technology Research Advancement Institution (BRAIN) (grant number: JPJ007097). This research was partially funded by the Scientific Research on Innovative Areas IBmS: JSPS KAKENHI (grant number: JP19H05771) and the Japan Society for the Promotion of Science, a Grant-in-Aid for Scientific Research B (grant number: JP21H00804).

Notes

The authors declare no competing financial interest.

ACKNOWLEDGMENTS

The authors thank MARUZEN-YUSHODO Co., Ltd. (<http://kw.maruzen.co.jp/kousei-honyaku/>) for English language editing.

ABBREVIATIONS

A β , amyloid β -peptide; **Ach**, acetylcholine; **AD**, Alzheimer's disease; **APP**, Amyloid precursor protein; **ARA**, arachidonic acid; **Arg**, arginine; **Asp**, aspartic acid; **α -T**, α -tocopherol; **β CAR**, β -carotene; **Cho**, cholesterol; **DHA**, docosahexaenoic acid; **ELISA**, enzyme-linked immunosorbent assay; **FA**, folate; **FBS**, fetal bovine serum; **FTIR**, Fourier transform infrared;

Glu, glutamic acid; **GAPDH**, glyceraldehyde-3-phosphate dehydrogenase; **IC₅₀**, effective concentrations at 50% value; **Ile**, isoleucine; **interleukin 1 beta**, IL1B; **IR**, infrared; **Leu**, leucine; **LNA**, linoleic acid; **LPC**, lysophosphatidylcholine; **LTN**, lutein; **Lys**, lysine; **Met**, methionine; **mRNA**, messenger ribonucleic acid; **MTT**, (3-(4,5-dimethylthiazol-2-yl)-2,5-diphenyltetrazolium bromide); **NANA**, sialic acid; **NC**, negative control; **NF- κ B**, nuclear factor-kappa B; **NFT**, neurofibrillary tangle; **NMDAR**, NMDA-type glutamate receptor; **OA**, oleic acid; **P/S**, penicillin/streptomycin; **PA**, palmitic acid; **PC**, phosphatidylcholine; **PE**, phosphatidylethanolamine; **PICUP**, photoinduced cross-linking of unmodified protein; **Phe**, phenylalanine; **Phe red**, phenol red; **PI**, phosphatidylinositol; **PMA**, paramethoxyamphetamine; **POA**, palmitoleic acid; **Ru[bpy]3Cl₂·6H₂O**, tris(2,2'-bipyridine)ruthenium(II) chloride hexahydrate; **RFU**, relative fluorescence unit; **ROS**, reactive oxygen species; **RT-qPCR**, quantitative real time polymerase chain reaction; **SA**, stearic acid; **SDS-PAGE**, sodium dodecyl sulfate polyacrylamide gel electrophoresis; **SE**, standard error; **Ser**, serine; **SM**, sphingomyelin; **Tau**, taurine; **TEM**, transmission electron microscopy; **ThT**, thioflavin T; **Thr**, threonine; **TNF**, tumor necrosis factor; **Tyr**, tyrosine; **V12**, vitamin B12; **VA**, retinol; **VBS**, pantothenic acid; **ZX**, zeaxanthin

REFERENCES

- (1) Li, X.; Feng, X.; Sun, X.; Hou, N.; Han, F.; Liu, Y. Global, Regional, and National Burden of Alzheimer's Disease and Other Dementias, 1990–2019. *Front. Aging Neurosci.* **2022**, *14*, 937486.
- (2) Tetsuka, S. Depression and Dementia in Older Adults: A Neuropsychological Review. *Aging Dis.* **2021**, *12* (8), 1920–1934.
- (3) Giacobini, E. Cholinesterase inhibitors: New roles and therapeutic alternatives. *Pharmacol. Res.* **2004**, *50*, 433–440.
- (4) Klafki, H.-W.; Staufienbiel, M.; Kornhuber, J.; Wiltfang, J. Therapeutic approaches to Alzheimer's disease. *Brain* **2006**, *129*, 2840–2855.
- (5) Farlow, M. R.; Cummings, J. L. Effective Pharmacologic Management of Alzheimer's Disease. *Am. J. Med.* **2007**, *120* (5), 388–397.
- (6) Chen, G.-F.; Xu, T.-H.; Yan, Y.; Zhou, Y.-R.; Jiang, Y.; Melcher, K.; Xu, H. E. Amyloid Beta: Structure, Biology and Structure-Based Therapeutic Development. *Acta Pharmacol. Sin.* **2017**, *38* (9), 1205–1235.
- (7) Selkoe, D. J. Alzheimer's disease results from the cerebral accumulation and cytotoxicity of amyloid β -protein. *J. Alzheimer's Dis.* **2001**, *3* (1), 75–80.
- (8) Chen, Z. L.; Singh, P. K.; Calvano, M.; Norris, E. H.; Strickland, S. A possible mechanism for the enhanced toxicity of beta-amyloid protofibrils in Alzheimer's disease. *Proc. Natl. Acad. Sci. U. S. A.* **2023**, *120*, No. e2309389120.
- (9) Walsh, D. M.; Selkoe, D. J. A β Oligomers – a decade of discovery. *J. Neurochem.* **2007**, *101* (5), 1172–1184.
- (10) Chong, Z. Z.; Li, F.; Maiese, K. Oxidative Stress in the Brain: Novel Cellular Targets That Govern Survival during Neurodegenerative Disease. *Prog. Neurobiol.* **2005**, *75* (3), 207–246.
- (11) Blennow, K.; de Leon, M. J.; Zetterberg, H. Alzheimer's Disease. *Lancet* **2006**, *368* (9533), 387–403.
- (12) Scheuner, D.; Eckman, C.; Jensen, M.; Song, X.; Citron, M.; Suzuki, N.; Bird, T. D.; Hardy, J.; Hutton, M.; Kukull, W.; Larson, E.; Levy-Lahad, L.; Viitanen, M.; Peskind, E.; Poorkaj, P.; Schellenberg, G.; Tanzi, R.; Wasco, W.; Lannfelt, L.; Selkoe, D.; Younkin, S. Secreted amyloid β -protein similar to that in the senile plaques of Alzheimer's disease is increased in vivo by the presenilin 1 and 2 and APP mutations linked to familial Alzheimer's disease. *Nat. Med.* **1996**, *2* (8), 864–870.

- (13) Chen, Z.-L.; Singh, P. K.; Calvano, M.; Norris, E. H.; Strickland, S. A Possible Mechanism for the Enhanced Toxicity of Beta-Amyloid Protofibrils in Alzheimer's Disease. *Proc. Natl. Acad. Sci. U.S.A.* **2023**, *120* (36), No. e2309389120.
- (14) Zhang, Y.; Chen, H.; Li, R.; Sterling, K.; Song, W. Amyloid β -based therapy for Alzheimer's disease: challenges, successes and future. *Signal Transduction Targeted Ther.* **2023**, *8* (1), 248.
- (15) Ylilauri, M. P.; Voutilainen, S.; Lönnroos, E.; Mursu, J.; Virtanen, H. E.; Koskinen, T. T.; Salonen, J. T.; Tuomainen, T.-P.; Virtanen, J. K. Association of Dietary Cholesterol and Egg Intakes with the Risk of Incident Dementia or Alzheimer Disease: The Kuopio Ischaemic Heart Disease Risk Factor Study. *Am. J. Clin. Nutr.* **2017**, *105* (2), 476–484.
- (16) Thomas, L. V.; Suzuki, K.; Zhao, J. Probiotics: A Proactive Approach to Health. A Symposium Report. *Br. J. Nutr.* **2015**, *114*, S1–S15.
- (17) Yamamoto, Y.; Kato, E.; Ando, A. Increased Antioxidative Activity of Ovalbumin by Heat Treating in an Emulsion of Linoleic Acid. *Biosci., Biotechnol., Biochem.* **1996**, *60* (9), 1430–1433.
- (18) Margara-Escudero, H. J.; Zamora-Ros, R.; de Villasante, I.; Crous-Bou, M.; Chirlaque, M.-D.; Amiano, P.; Mar, J.; Barricarte, A.; Ardanaz, E.; Huerta, J. M. Association Between Egg Consumption and Dementia Risk in the EPIC-Spain Dementia Cohort. *Front. Nutr.* **2022**, *9*, 827307.
- (19) Ono, K.; Li, L.; Takamura, Y.; Yoshiike, Y.; Zhu, L.; Han, F.; Mao, X.; Ikeda, T.; Takasaki, J.-I.; Nishijo, H.; Takashima, A.; Teplow, D. B.; Zagorski, M. G.; Yamada, M. Phenolic Compounds Prevent Amyloid β -Protein Oligomerization and Synaptic Dysfunction by Site-specific Binding. *J. Biol. Chem.* **2012**, *287* (18), 14631–14643.
- (20) Bitan, G.; Tarus, B.; Vollers, S. S.; Lashuel, H. A.; Condrón, M. M.; Straub, J. E.; Teplow, D. B. A Molecular Switch in Amyloid Assembly: Met³⁵ and Amyloid β -Protein Oligomerization. *J. Am. Chem. Soc.* **2003**, *125* (50), 15359–15365.
- (21) Zhaliakza, K.; Kurouski, D. Nanoscale Characterization of Parallel and Antiparallel β -Sheet Amyloid Beta 1–42 Aggregates. *ACS Chem. Neurosci.* **2022**, *13* (19), 2813–2820.
- (22) Sarroukh, R.; Goormaghtigh, E.; Ruysschaert, J.-M.; Raussens, V. ATR-FTIR: A “Rejuvenated” Tool to Investigate Amyloid Proteins. *Biochim. Biophys. Acta* **2013**, *1828* (10), 2328–2338.
- (23) El Shatshat, A.; Pham, A. T.; Rao, P. P. N. Interactions of polyunsaturated fatty acids with amyloid peptides A β 40 and A β 42. *Arch. Biochem. Biophys.* **2019**, *663*, 34–43.
- (24) Shen, L.; Adachi, T.; Vanden Bout, D.; Zhu, X.-Y. A Mobile Precursor Determines Amyloid- β Peptide Fibril Formation at Interfaces. *J. Am. Chem. Soc.* **2012**, *134* (34), 14172–14178.
- (25) Srivastava, A. K.; Pittman, J. M.; Zerweck, J.; Venkata, B. S.; Moore, P. C.; Sachleben, J. R.; Meredith, S. C. β -Amyloid Aggregation and Heterogeneous Nucleation. *Protein Sci.* **2019**, *28* (9), 1567–1581.
- (26) Sheikh, A. M.; Nagai, A. Lysophosphatidylcholine Modulates Fibril Formation of Amyloid Beta Peptide. *FEBS J.* **2011**, *278* (4), 634–642.
- (27) Katayama, S.; Ogawa, H.; Nakamura, S. Apricot Carotenoids Possess Potent Anti-Amyloidogenic Activity in Vitro. *J. Agric. Food Chem.* **2011**, *59* (23), 12691–12696.
- (28) Long, J. M.; Holtzman, D. M. Alzheimer Disease: An Update on Pathobiology and Treatment Strategies. *Cell* **2019**, *179* (2), 312–339.
- (29) Yang, J. H.; Lee, E. O.; Kim, S. E.; Suh, Y.-H.; Chong, Y. H. Norepinephrine differentially modulates the innate inflammatory response provoked by amyloid- β peptide via action at β -adrenoceptors and activation of cAMP/PKA pathway in human THP-1 macrophages. *Exp. Neurol.* **2012**, *236* (2), 199–206.
- (30) An, Y. W.; Jhang, K. A.; Woo, S.-Y.; Kang, J. L.; Chong, Y. H. Sulforaphane exerts its anti-inflammatory effect against amyloid- β peptide via STAT-1 dephosphorylation and activation of Nrf2/HO-1 cascade in human THP-1 macrophages. *Neurobiol. Aging* **2016**, *38*, 1–10.
- (31) Shukuri, M.; Mawatari, A.; Ohno, M.; Suzuki, M.; Doi, H.; Watanabe, Y.; Onoe, H. Detection of Cyclooxygenase-1 in Activated Microglia During Amyloid Plaque Progression: PET Studies in Alzheimer's Disease Model Mice. *J. Nucl. Med.* **2016**, *57* (2), 291–296.
- (32) Tokuda, H.; Horikawa, C.; Nishita, Y.; Nakamura, A.; Kato, T.; Kaneda, Y.; Obata, H.; Rogi, T.; Nakai, M.; Shimokata, H.; Otsuka, R. The Association between Long-Chain Polyunsaturated Fatty Acid Intake and Changes in Brain Volumes among Older Community-Dwelling Japanese People. *Neurobiol. Aging* **2022**, *117*, 179–188.
- (33) Mrowicka, M.; Mrowicki, J.; Kucharska, E.; Majsterek, I. Lutein and Zeaxanthin and Their Roles in Age-Related Macular Degeneration-Neurodegenerative Disease. *Nutrients* **2022**, *14* (4), 827.
- (34) Schweiggert, R. M.; Carle, R. Carotenoid Deposition in Plant and Animal Foods and Its Impact on Bioavailability. *Crit. Rev. Food Sci. Nutr.* **2017**, *57* (9), 1807–1830.
- (35) Shin, H. S.; Kim, J. W.; Kim, J. H.; Lee, D. G.; Lee, S.; Kil, D. Y. Effect of Feeding Duration of Diets Containing Corn Distillers Dried Grains with Solubles on Productive Performance, Egg Quality, and Lutein and Zeaxanthin Concentrations of Egg Yolk in Laying Hens. *Poult. Sci.* **2016**, *95* (10), 2366–2371.
- (36) Richelle, M.; Enslin, M.; Hager, C.; Groux, M.; Tavazzi, I.; Godin, J.-P.; Berger, A.; Métairon, S.; Quaille, S.; Pigué-Welsch, C.; Sagalowicz, L.; Green, H.; Fay, L. B. Both free and esterified plant sterols reduce cholesterol absorption and the bioavailability of β -carotene and α -tocopherol in normocholesterolemic humans. *Am. J. Clin. Nutr.* **2004**, *80* (1), 171–177.
- (37) Sugawara, T.; Kushiro, M.; Zhang, H.; Ono, H.; Nagao, A.; Nara, E. Lysophosphatidylcholine Enhances Carotenoid Uptake from Mixed Micelles by Caco-2 Human Intestinal Cells. *J. Nutr.* **2001**, *131* (11), 2921–2927.
- (38) Vishwanathan, R.; Neuringer, M.; Snodderly, D. M.; Schalch, W.; Johnson, E. J. Macular Lutein and Zeaxanthin Are Related to Brain Lutein and Zeaxanthin in Primates. *Nutr. Neurosci.* **2013**, *16* (1), 21–29.